Delayed spectrum of two-level resonance fluorescence

X. Y. Huang,* R. Tanaś,† and J. H. Eberly
Department of Physics and Astronomy, University of Rochester, Rochester, New York 14627
(Received 5 January 1982)

We compute the time-dependent spectrum of fluorescence by two-level atoms after a strong resonant exciting laser pulse is turned off abruptly. The behavior of the "delayed" three-peaked spectrum is shown to be dependent on the natural lifetime of the upper state and on the bandwidth of the interferometer used in the measurement. A prompt increase in the central-peak intensity and an oscillating decay in the two side peaks are predicted to occur immediately after the laser is turned off. These are manifestations of the "undressing" of the atomic states. Our calculation permits consideration of the question of the speed of the undressing and its observation.

I. INTRODUCTION

We consider here resonance fluorescence of a two-level atom which is exposed to a strong resonant laser pulse for some time t_p and then for $t > t_p$ evolves freely. In other words, we assume the laser pulse to be switched on at $t=0$ and switched off at $t=t_p$. The subject of concern is the time-dependent fluorescence spectrum of such an atom, measured at times $t > t_p$. A schematic diagram of the experiment is shown in Fig. 1. We use the Eberly-Wodkiewicz counting-rate definition of the time-dependent physical spectrum.[1] The corresponding results while the atom is in the field have been obtained previously by Eberly, Kunasz, and Wodkiewicz.[2] It is well known that in the strong-field limit the resonance fluorescence spectrum has a three-peak structure and it is interesting to know how this structure evolves in time after the laser field is switched off.

II. EQUATIONS OF MOTION

We use here, as far as we can, the notation of Eberly, Kunasz, and Wodkiewicz[2] (EKW). We define atomic variables, in the Heisenberg picture and the rotating coordinate system, in the usual way:

$$\hat{W}=\hat{\sigma}_{22}-\hat{\sigma}_{11}\,, \tag{2.1}$$

$$\hat{S}_{12}=\hat{\sigma}_{12}e^{i\omega_l t}\,, \tag{2.2}$$

$$\hat{S}_{21}=\hat{\sigma}_{21}e^{-i\omega_l t}\,. \tag{2.3}$$

With this definition the equations of motion can be written in matrix form:

$$\frac{d\hat{\psi}}{dt}=M\hat{\psi}+\hat{f}\,, \tag{2.4}$$

where

$$\hat{\psi}=\begin{bmatrix}\hat{S}_{21}\\ \hat{W}\\ \hat{S}_{12}\end{bmatrix},\quad \hat{f}=\begin{bmatrix}0\\ -A\\ 0\end{bmatrix}, \tag{2.5}$$

$$M=\begin{bmatrix}-A/2+i\Delta & i/2\Omega & 0\\ i\Omega & -A & -i\Omega\\ 0 & -i/2\Omega & -A/2-i\Delta\end{bmatrix}. \tag{2.6}$$

Here A is the Einstein coefficient of spontaneous emission (i.e., $A=1/\tau_0$, where τ_0 is the lifetime of the upper level, Δ is the detuning of the laser below the atomic resonance, $\Delta=\omega_{21}-\omega_l$, and Ω is the Rabi frequency: $\Omega=(2/\hbar)\vec{d}_{21}\cdot\vec{E}_0$, where $\vec{d}_{21}$ is the transition dipole matrix element, and the electric field strength is written

$$\vec{E}(t)=\vec{E}_0\exp(-i\omega_l t)+\text{c.c.}$$

To calculate the spectrum of resonance fluorescence we need the dipole-dipole correlation operator

$$\hat{\sigma}_{21}(t_1)\hat{\sigma}_{12}(t_2)=\hat{S}_{21}(t_1)\hat{S}_{12}(t_2)\exp[i\omega_l(t_1-t_2)]\,. \tag{2.7}$$

Following Milonni,[2,3] we obtain the expectation value of this operator from the coupled equations for the expectation values of the three operator

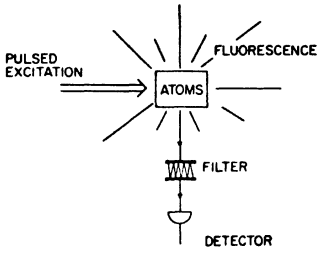

FIG. 1. Schematic diagram of resonance fluorescence experiment.

products $\hat{S}_{21}(t_1)\hat{S}_{12}(t_2)$, $\hat{W}(t_1)\hat{S}_{12}(t_2)$, and $\hat{S}_{12}(t_1)\hat{S}_{12}(t_2)$.

For an atom in the field we can write the result in matrix form, with the same matrix M given in (2.6), as follows:

$$\frac{d\hat{\Psi}(t_1,t_2)}{dt_1}=M\hat{\Psi}(t_1,t_2)+\hat{F}\ , \tag{2.8}$$

where now

$$\hat{\Psi}(t_1,t_2)=\begin{bmatrix}\hat{S}_{21}(t_1)\hat{S}_{12}(t_2)\\ \hat{W}(t_1)\hat{S}_{12}(t_2)\\ \hat{S}_{12}(t_1)\hat{S}_{12}(t_2)\end{bmatrix}\ ,$$

$$\hat{F}=\begin{bmatrix}0\\ -A\hat{S}_{12}(t_2)\\ 0\end{bmatrix}\ . \tag{2.9}$$

For an atom out of the field the above equations can be written in the same form, by changing the matrix M into the diagonal matrix $M_0=M(\Omega=0)$. To calculate the time-dependent spectrum both t_1 and t_2 dependences will be needed. We are concerned with expectation values of these operator quantities, which we denote as quantities without the circumflex

$$\psi(t)=\mathrm{Tr}[\rho_{\mathrm{atom}}(0)\otimes\rho_{\mathrm{field}}(0)\hat{\psi}(t)]\ , \tag{2.10a}$$

$$\Psi(t_1,t_2)=\mathrm{Tr}[\rho_{\mathrm{atom}}(0)\otimes\rho_{\mathrm{field}}(0)\hat{\Psi}(t_1,t_2)]\ . \tag{2.10b}$$

The solutions to (2.4) and (2.8) are easily written in terms of the matrix M or M_0 depending on whether the atom is in or out of the field. We give some of the details in the Appendix.

III. TIME-DEPENDENT PHYSICAL SPECTRUM OF DELAYED RESONANCE FLUORESCENCE

According to the definition of the time-dependent physical spectrum,[1] we must evaluate (for $t\geq 0$)

$$\mathscr{S}(t,\omega,\Gamma)=\Gamma\int_0^t dt_1\int_0^t dt_2 e^{-(\Gamma/2-iD)(t-t_1)}e^{-(\Gamma/2+iD)(t-t_2)}\langle\hat{S}_{21}(t_1)\hat{S}_{12}(t_2)\rangle\ . \tag{3.1}$$

Here Γ is the bandwidth of the ideal Fabry-Perot interferometer which has its transmission peak at frequency ω. The detuning of the laser from the interferometer is denoted $D\equiv\omega-\omega_l$. This spectrum can be written as the first component of a time- and frequency-dependent vector S:

$$S(t,\omega,\Gamma)=\Gamma\int_0^t dt_1\int_0^t dt_2 e^{-(\Gamma/2-iD)(t-t_1)}e^{-(\Gamma/2+iD)(t-t_2)}\Psi(t_1,t_2)\ . \tag{3.2}$$

The double integration in (3.2) can be divided into three different regions as shown in Fig. 2. In region I both integrations are over the interval $0\leq t\leq t_p$, when the atom is in the field and its evolution is governed by the matrix M. In region III the atom is out of the field and its evolution is due to the matrix M_0. Finally, in region II, which is composed of two parts (complex conjugate to each other), one integration is over the time when the atom is in the field and the other when the atom is out of the field. In this mixed term the atomic evolution is due to either the matrix M or M_0 depending on whether the atom is in or out of the field. Upon taking into account these different regions of the time integration, the time-dependent spectrum of resonance fluorescence, as given by (3.2), can be split into three separate parts:

$$S(t,\omega,\Gamma)=S_{\mathrm{I}}(t,\omega,\Gamma)+S_{\mathrm{II}}(t,\omega,\Gamma)+S_{\mathrm{III}}(t,\omega,\Gamma)\ . \tag{3.3}$$

We can write these three parts as follows:

$$\begin{aligned}S_{\mathrm{I}}(t,\omega,\Gamma)&=\Gamma\int_0^{t_p}dt_1\int_0^{t_p}dt_2 e^{-(\Gamma/2-iD)(t-t_1)}e^{-(\Gamma/2+iD)(t-t_2)}\Psi(t_1,t_2)\\&=e^{-\Gamma(t-t_p)}2\Gamma\,\mathrm{Re}\int_0^{t_p}dt_2 e^{-\Gamma(t_p-t_2)}\int_0^{t_p-t_2}d\tau e^{(\Gamma/2+iD)\tau}\Psi(t_2,\tau)\ ,\end{aligned} \tag{3.4}$$

$$\begin{aligned}S_{\mathrm{II}}(t,\omega,\Gamma)&=2\Gamma\,\mathrm{Re}\int_{t_p}^t dt_1\int_0^{t_p}dt_2 e^{-(\Gamma/2-iD)(t-t_1)}e^{-(\Gamma/2+iD)(t-t_2)}\Psi(t_1,t_2)\\&=2\Gamma\,\mathrm{Re}\int_0^{t-t_p}dt_1\int_0^{t_p}dt_2 e^{-(\Gamma/2-iD)(t-t_p-t_1)}e^{-(\Gamma/2+iD)(t-t_2)}\Psi(t_p+t_1,t_2)\ ,\end{aligned} \tag{3.5}$$

and

$$\begin{aligned}S_{\mathrm{III}}(t,\omega,\Gamma)&=\Gamma\int_{t_p}^t dt_1\int_{t_p}^t dt_2 e^{-(\Gamma/2-iD)(t-t_1)}e^{-(\Gamma/2+iD)(t-t_2)}\Psi(t_1,t_2)\\&=2\Gamma\,\mathrm{Re}\int_0^{t-t_p}dt_2 e^{-\Gamma(t-t_p-t_2)}\int_0^{t-t_p-t_2}d\tau e^{(\Gamma/2-iD)\tau}\Psi(t_p+t_2+\tau,t_p+t_2)\ .\end{aligned} \tag{3.6}$$

All time dependences in Eqs. (3.4)–(3.6) are of the exponential type as given by (A1) and (A2) with the proper matrix M or M_0 as well as the corresponding initial conditions. All integrations can be performed explicitly, as in EKW, and for S_{I} their result is obtained, except for the multiplication of an additional overall decay factor $e^{-\Gamma(t-t_p)}$, where $t-t_p$ is the delay time, i.e., the time which has elapsed since the laser was switched off.

The second and third contributions can be evaluated explicitly also, and are given in terms of the matrices M and M_0 in the Appendix. Using the formulas we have found for S_{I}, S_{II}, and S_{III}, the spectrum can easily be evaluated numerically. There is a wide variety of parameters that the spectrum depends on. To exhibit the spectrum as a function of all of them is not possible to do briefly. Here we will restrict our attention only to the case of exact resonance and strong excitation, in the long-excitation limit.

IV. RESONANT EXCITATION BY A STRONG FIELD

If the laser frequency ω_l is tuned exactly to the atomic transition frequency ω_{21} ($\Delta=\omega_{21}-\omega_l=0$), the laser intensity is strong ($\Omega \gg A$), and the pulse duration is long enough so that we can put $t_p \to \infty$, with $t-t_p$ finite, the spectrum (3.1) has the explicit form

$$
\begin{aligned}
\mathcal{S}(t,\omega,\Gamma)=\tfrac{1}{4}e^{-\Gamma(t-t_p)}\Bigg[& \frac{\Gamma/2+\frac{3}{4}A}{(D-\Omega)^2+(\Gamma/2+\tfrac{3}{4}A)^2}+\frac{\Gamma+A}{D^2+\frac{1}{4}(\Gamma+A)^2}+\frac{\Gamma/2+\frac{3}{4}A}{(D+\Omega)^2+(\Gamma/2+\tfrac{3}{4}A)^2} \\
& +\left[\frac{A}{\Omega}\right]^2\frac{\Gamma}{D^2+(\Gamma/2)^2}\Bigg]+\frac{\Gamma}{8}\frac{e^{-(1/2)(\Gamma+A)(t-t_p)}\cos D(t-t_p)-e^{-\Gamma(t-t_p)}}{D^2+\frac{1}{4}(\Gamma-A)^2} \\
\times\Bigg[& \frac{(\Gamma/2+\frac{3}{4}A)(\Gamma-A)+2D(D-\Omega)}{(D-\Omega)^2+(\Gamma/2+\tfrac{3}{4}A)^2}+\frac{(\Gamma+A)(\Gamma-A)+(2D)^2}{D^2+\frac{1}{4}(\Gamma+A)^2} \\
& +\frac{(\Gamma/2+\frac{3}{4}A)(\Gamma-A)+2D(D+\Omega)}{(D+\Omega)^2+(\Gamma/2+\tfrac{3}{4}A)^2}+\left[\frac{A}{\Omega}\right]^2\frac{\Gamma(\Gamma-A)+(2D)^2}{D^2+(\Gamma/2)^2}\Bigg] \\
+\frac{\Gamma}{8}\frac{e^{-(1/2)(\Gamma+A)(t-t_p)}\sin D(t-t_p)}{D^2+\frac{1}{4}(\Gamma-A)^2} & \\
\times\Bigg[& \frac{2D(\Gamma/2+\frac{3}{4}A)-(\Gamma-A)(D-\Omega)}{(D-\Omega)^2+(\Gamma/2+\tfrac{3}{4}A)^2}+\frac{4DA}{D^2+\frac{1}{4}(\Gamma+A)^2} \\
& +\frac{2D(\Gamma/2+\frac{3}{4}A)-(\Gamma-A)(D+\Omega)}{(D+\Omega)^2+(\Gamma/2+\tfrac{3}{4}A)^2}+\left[\frac{A}{\Omega}\right]^2\frac{2DA}{D^2+(\Gamma/2)^2}\Bigg] \\
+\Bigg[& \Gamma\frac{e^{-A(t-t_p)}-e^{-(1/2)(\Gamma+A)(t-t_p)}\cos D(t-t_p)}{D^2+\frac{1}{4}(\Gamma-A)^2}-\frac{\Gamma}{2}\frac{e^{-A(t-t_p)}-e^{-\Gamma(t-t_p)}}{D^2+\frac{1}{4}(\Gamma-A)^2}\Bigg]. \qquad (4.1)
\end{aligned}
$$

Note that the first square bracket contains the familiar steady-state three-peaked spectrum,[4] including the coherent scattering "delta function" as the fourth term. Here the delta function is a Lorentzian because our theory includes the influence of the interferometer on the spectrum. This term is damped in a natural way.

The second and third terms are new contribu-

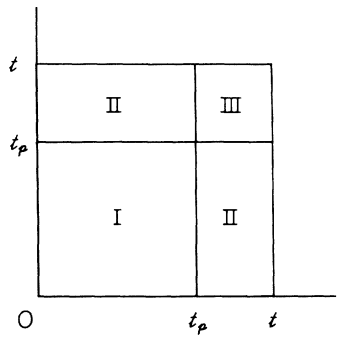

FIG. 2. Regions of time integrations. t_p is the time duration of laser pulse.

tions. They arise from region II of the time integrations. These two terms reflect both the features of the three-peak steady-state spectrum, which can be recognized in the denominators of the terms in the brackets, and the spontaneous emission spectrum, which can be associated with the extra resonant factor in front of the brackets as well as the modulation terms. Because of this extra resonant factor which depends on $\Gamma-A$ these terms contribute significantly to the spectrum when $\Gamma\approx A$. The time modulation in the side peaks then becomes visible.[5]

The fourth term is simply the spontaneous emission spectrum of EKW, the linewidth of which is also described by the difference $\Gamma-A$.

The time-dependent spectrum described by these four terms is illustrated in the following figures for different values of Γ/A (Fig. 3). The spectrum is the three-peak spectrum, as it should be, in the strong field. For $\Gamma/A \ll 1$, i.e., for a narrow-bandwidth interferometer, this three-peak structure is clearly resolved [Fig. 3(a)]. The central peak and the side peaks decay in time with the same rate, determined by the interferometer bandwidth Γ, and the oscillating terms do not contribute significantly to the spectrum. As Γ becomes comparable to A [Figs. 3(b)–3(d)], the time-dependent spectrum changes significantly. The side peaks now decay much faster than the central peak. The oscillating terms are more pronounced and are clearly visible in the side peaks. Also one can observe the temporary increase in height of the central peak to be relatively much greater than in the narrow-bandwidth interferometer case. This sudden increase has been found by Saari[6] in a calculation of the far-off-resonance Rayleigh line shape in the weak-field case, and by Courtens and Szöke,[7] in a calculation for time-dependent fluorescence when an adiabatic square driving pulse terminates [see Fig. 3(b) of Ref. 7]. It has not been observed experimentally to the best of our knowledge. We discuss its meaning in Sec. V. The time dependence of the central peak as well as the side peaks for different values of Γ/A are shown in more detail in Fig. 4.

V. STRONG-FIELD LIMITS

There are two interesting limits which can be derived from our formula (4.1). In the strong-field case ($\Omega \gg A,\Gamma$) we can obtain from (4.1) the approximate formulas describing the time dependence of the height of the central peak $H_0(t)$ as well as of the side peaks $H_\pm(t)$:

$$H_0(t)=\frac{1}{(\Gamma-A)^2}\left[(\Gamma+A)e^{-\Gamma(t-t_p)}+2\Gamma e^{-A(t-t_p)}-2\Gamma\frac{\Gamma+3A}{\Gamma+A}e^{-\frac{1}{2}(\Gamma+A)(t-t_p)}\right], \tag{5.1}$$

$$H_\pm(t)=\frac{1}{4}\frac{1}{\Gamma/2+\frac{3}{4}A}e^{-\Gamma(t-t_p)}. \tag{5.2}$$

There are two complementary limits to consider:

(i) We have a narrow-band interferometer ($\Gamma \ll A$), where we have

$$H_0(t)\approx\frac{1}{A}e^{-\Gamma(t-t_p)}, \tag{5.3}$$

$$H_\pm(t)\approx\frac{1}{3A}e^{-\Gamma(t-t_p)}. \tag{5.4}$$

Formulas (5.3) and (5.4) explain the time behavior of the spectrum as shown in Fig. 3(a). Both central and side peaks decay with the rate constant of the interferometer and the ratio 3:1 in the heights of the peaks is preserved. The peak amplitudes are proportional to A^{-1}.

(ii) We have a broad-band interferometer ($\Gamma \gg A$), where we have

$$H_0(t)\approx\frac{1}{\Gamma}(e^{-\Gamma(t-t_p)}-2e^{-(\Gamma/2)(t-t_p)}+2e^{-A(t-t_p)}), \tag{5.5}$$

$$H_\pm(t)\approx\frac{1}{2\Gamma}e^{-\Gamma(t-t_p)}. \tag{5.6}$$

In this case the side peaks decay very rapidly, as given by Eq. (5.6). The central peak shows more complicated behavior. For $t-t_p \ll \Gamma^{-1},A^{-1}$, the height of the central peak is Γ^{-1}. For $\Gamma^{-1}\approx t-t_p \ll A^{-1}$, the height of the peak reaches its maximum $H_0=2/\Gamma$, which is twice the height at time $t-t_p=0$. For time $t-t_p \gtrsim \Gamma^{-1}$, the peak starts to decay with the decay constant A. The ratio

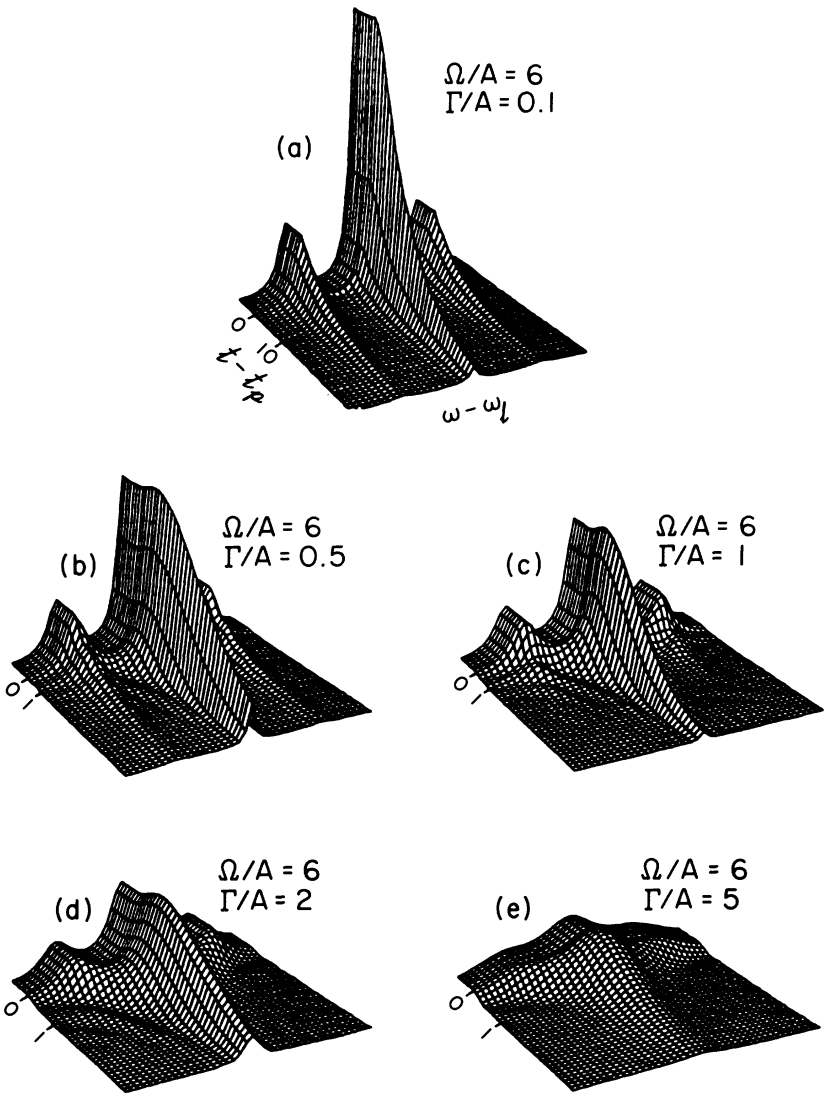

FIG. 3. Dealyed resonance fluorescence spectrum for $\Omega/A=6$ and different values of Γ/A: (a) $\Gamma/A=0.1$, (b) $\Gamma/A=0.5$, (c) $\Gamma/A=1$, (d) $\Gamma/A=2$, (e) $\Gamma/A=5$. First few lines in the time direction represent the steady-state spectrum for easier reference. Time is in units of A^{-1}. Labeling of the curves in graph (a) applies to (b)—(e).

of the height of the central peak to the side peak at $t=t_p$ is 2:1 and the amplitudes are proportional to Γ^{-1}. These features of the time-dependent spectrum of resonance fluorescence are illustrated in Figs. 5 and 6. As Γ increases, the amplitudes of the peaks decrease [see (5.5) and (5.6)] and we can see the relative increase of the central peak shown in Fig. 6 to be close to the factor of 2.

The initial character of the relative increase of the central peak can be obtained independent of Γ and A by an expansion of $H_0(t)$ in powers of $t-t_p$. From Eq. (5.1) we find

$$H_0(t)=\frac{1}{\Gamma+A}+\frac{\Gamma}{4}(t-t_p)^2+O((t-t_p)^3)\ . \qquad (5.7)$$

Spectral line features in Figs. 4(a) and 6 are in agreement with this result.

VI. EXTREMELY BROAD-BANDWIDTH INTERFEROMETER

Our formalism also permits a discussion of very fast (broad-bandwidth) detectors. We consider in

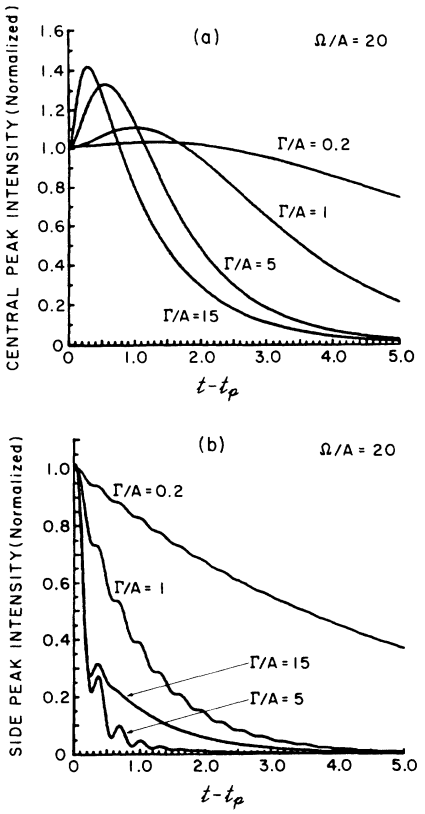

FIG. 4. Time dependence of the central and side peaks for $\Omega/A=20$ and several values of Γ/A: $\Gamma/A=0.2$, 1, 5, 15. x coordinate denotes delay time $t-t_p$ in units of A^{-1}: $x=A(t-t_p)$, and y coordinate denotes normalized spectral peak intensity: $y=S(t,\omega,\Gamma)/S(t_p,\omega,\Gamma)$, where $\omega=\omega_l$ for the central peak and $\omega=\omega_l\pm\Omega$ for the side peak.

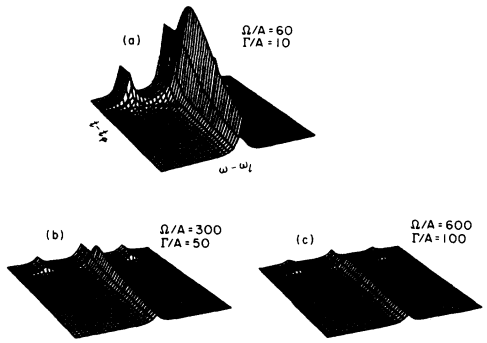

FIG. 5. Spectrum obtained using a broad-band interferometer for different values of parameters: (a) $\Omega/A=60$, $\Gamma/A=10$; (b) $\Omega/A=300$, $\Gamma/A=50$; (c) $\Omega/A=600$, $\Gamma/A=100$. Amplitude scale has been multiplied by a factor of 5 as compared to Fig. 3. The labeling of the curves in (a) applies to (b) and (c).

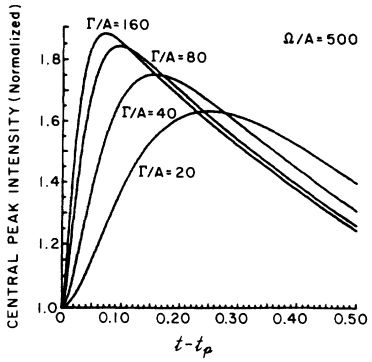

FIG. 6. Time dependence of the normalized central-peak intensity for the case of the broad-band interferometer for various values of parameters: $\Gamma/A=20$, 40, 80, 160, and $\Omega/A=500$. Meaning of the coordinates is the same as in Fig. 4.

this section the case of a very broad-band interferometer, for which $\Gamma\gg\Omega$.

Equation (4.1) and the limit of $\Gamma\gg\Omega\gg A$ leads to a quite simple expression for the delayed physical spectrum for a two-level system as follows:

$$\mathcal{S}(t,\omega,\Gamma)\approx\frac{2}{\Gamma}e^{-A(t-t_p)}\,. \tag{6.1}$$

In (6.1) the dependence on the detuning D and the differences between the central peak and side peaks in the spectrum disappear. The overall decay behavior is just determined by the lifetime of the upper state of the system.

By comparing (6.1) with (5.2), we find the normalized side-peak intensity $H_{\pm,\mathrm{norm}}(t)$ defined in Fig. 4 can be written as

$$H_{\pm,\mathrm{norm}}(t)\approx e^{-\Gamma(t-t_p)},\quad \text{for } \Omega\gg\Gamma,A \tag{6.2}$$

and

$$H_{\pm,\mathrm{norm}}(t)\approx e^{-A(t-t_p)},\quad \text{for } \Gamma\gg\Omega\gg A\,. \tag{6.3}$$

There is a wide difference in time decay behavior for the side peaks in these two limits. In scanning the values of Γ from $\Gamma\ll\Omega$ to $\Gamma\gg\Omega$, we find there is a critical value Γ_c. In the cases with $\Gamma<\Gamma_c$, the normalized side-peak intensity $H_{\pm,\mathrm{norm}}(t)$ will decay faster with larger Γ, but in the cases with $\Gamma>\Gamma_c$, $H_{\pm,\mathrm{norm}}(t)$ will decay more slowly with larger Γ values.

By inspection of the time decay behavior for the side peaks with various values of Γ/A for $\Omega/A=20$ in Figs. 4(b) and 7, we find the critical value for Γ around $\Gamma_c/A\approx5$. A more detailed inspection of neighboring values shows that $\Gamma_c/A\simeq7$ for the case

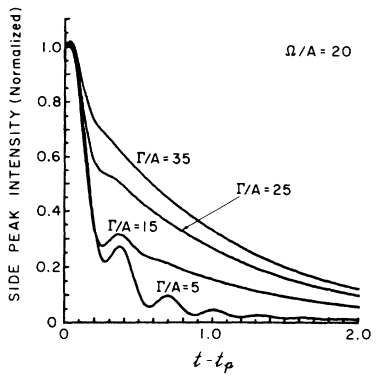

FIG. 7. Time dependence of the normalized side-peak intensity for $\Omega/A=20$ and $\Gamma/A=5$, 15, 25, 35. Meaning of the coordinate is the same as Fig. 4.

of $\Omega/A=20$.

The physical reason for the changing decay behavior is obvious. For the extremely broad-bandwidth interferometer cases $\Gamma/A \gtrsim \Omega/A \gg 1$, the central and side peaks in the spectrum are dominated by the instrumental width Γ, and the three peaks in the spectrum completely overlap each other. The power that we measure at the side peaks is partially due to the power of the central peak. This is why the time decay phenomena for the side peaks will depart from $e^{-\Gamma(t-t_p)}$. We can also find from (6.1) that neither the sudden increase in height of the central peak nor the fast decay of the side peaks will be preserved in the cases of extremely fast response filters.

VII. POWER "TRANSFER" PROCESSES BETWEEN SPECTRAL PEAKS

In the case of the strong-field $\Omega \gg \Gamma, A$, the spectral lines of the three peaks are resolved clearly even for a "bad" interferometer ($\Gamma \gg A$). Terms corresponding to the central and side peaks are easy to separate in Eq. (4.1). We perform the integration over detuning D from $-\infty$ to $+\infty$, treating the terms belonging to the central peak and side peaks separately. We obtain the total power of the central peak P_0 and side peaks $P_\pm$ correspondingly (i.e., the "area" under the spectral lines in each peak):

$$P_0(t)=\frac{\pi}{2}e^{-\Gamma(t-t_p)}+\pi\frac{\Gamma}{\Gamma-A}(e^{-A(t-t_p)}-e^{-\Gamma(t-t_p)}), \tag{7.1}$$

$$P_\pm(t)=\frac{\pi}{4}e^{-\Gamma(t-t_p)}. \tag{7.2}$$

It is interesting to note that in these expressions for spectral power the oscillation terms like $\cos D(t-t_p)$ and $\sin D(t-t_p)$ are absent, and the power of the spectral peaks decays monotonously.

For times immediately after the laser turned off, some cancellations occur in (7.1). For $t-t_p \ll A^{-1}, \Gamma^{-1}$ we find the power in the central peak and the side peaks to be

$$P_0(t)\approx\frac{\pi}{2}[1+\Gamma(t-t_p)], \tag{7.3}$$

$$P_\pm(t)\approx\frac{\pi}{4}[1-\Gamma(t-t_p)]. \tag{7.4}$$

Note that the sum of the power in the two side peaks is equal to the power in the central peak. This is well known to be the case before the laser turned off.[4] Note also that the time derivative of P_0 is positive, indicating a power transfer toward the central peak.

We discuss the power transfer between the spectral peaks in two limits:

(i) For the narrow-band interferometer ($\Gamma \ll A$),

$$P_0(t)\approx\frac{\pi}{2}e^{-\Gamma(t-t_p)}, \tag{7.5}$$

$$P_\pm(t)\approx\frac{\pi}{4}e^{-\Gamma(t-t_p)}. \tag{7.6}$$

(ii) For the broad-band interferometer ($\Gamma \gg A$),

$$\left.\begin{aligned} &P_0(t)\approx\pi e^{-A(t-t_p)}, && (7.7)\\ &P_\pm(t)\approx 0. && (7.8)\end{aligned}\right\} \text{ for } t-t_p \geq \Gamma^{-1}$$

For a narrow-band interferometer, the power of both central and side peaks decays exponentially with the slow rate constant Γ^{-1}. In broad-band interferometer cases ($\Gamma \gg A$), the power of the side peaks decays more rapidly than the central peak. For $\Gamma^{-1} \lesssim t-t_p \ll A^{-1}$ the power of the central peak can jump to a maximum which is twice the initial power value. This behavior can be explained as a transfer of the power which was associated with the two side peaks into the central peak after the laser pulse is switched off suddenly. The faster time response of the broad-band interferometer makes the power transfer processes observable (because the interferometer does not store for long light emitted into it by the atoms before the laser was switched off). The increase in the height of the central peak mentioned in Sec. V is closely related to such power transfer processes.

VIII. COMMENTS

We have made a calculation, in the resonant strong-field limit, of the delayed time-dependent

resonance fluorescence spectrum of a two-level system, taking the response feature of the interferometer into account. For measuring the time-dependence of the three resolved peaks, the condition $\Omega \gg \Gamma \gg A$ is appropriate.

When a constant driving field of long duration terminates suddenly, the ac Stark splitting of the upper and lower levels disappears, and the population in these dressed sublevels transfers to the bare (field-free) levels. This process of undressing is, in principle, very fast, and is interesting to consider carefully. The resonance fluorescence spectrum is, of course, sensitive to the populations of the different dressed levels, and thus the spectrum offers a method of observing undressing.

Our calculation shows in a rather transparent way the limitations inherent in such a measurement, which are not unexpected. Section V shows that a broad-band interferometer can observe the undressing by measuring, for example, the prompt increase in central-peak height after the laser turns off. This is related to the power transfer of Sec. VII. However, Sec. VI shows that any attempt to observe a "fundamental" limit on the speed of the undressing, by making the interferometer respond faster (by increasing Γ), must fail as soon as Γ becomes comparable with Ω. This is because the interferometer then fails to distinguish the side peaks from the center peak. One can say, therefore, that the undressing cannot, in principle, be observed to occur faster than the Rabi frequency, no matter how rapidly the laser is turned off.

Williams *et al.*[8] made a direct measurement of the scattering lifetime in molecular iodine as a function of the incident excitation frequency. When the excitation was on resonance, they observed a spectral lifetime of about 1 μsec, which is the natural fluorescence lifetime of the upper excited state. When the frequency was moved off resonance, the scattering became very short, and hence "Raman-type" (see Fig. 1 of Ref. 7). The time-dependent behavior of the spectrum that they experimentally observed in the resonance case is in agreement with our "prompt" results for the central peak [see Figs. 4(a) and 6]. As they used a rather weak laser pulse in their experiment, a sudden increase in height of the spectrum was not observed.

Finally, although the working expressions presented here in Sec. IV are valid only for monochromatic strong fields and exact resonance, they are explicit and fully analytic. Also, they are not really restricted to the case of a nonadiabatic turning off of the pulse, because of the integrating character of the interferometer. Of course the solutions given in the Appendix are exact and can be applied on and off resonance and for weak or strong fields. Rather than pursing the numerical study of these solutions in all their complexity it seems more interesting to study next the opposite limit to the present one. In a subsequent note we will discuss weak nonmonochromatic fields, possibly far from resonance. We will explore the connections with the work of Saari,[6] Courtens and Szöke,[7] Knight, Molander, and Stroud,[9] and Raymer and Cooper.[10]

ACKNOWLEDGMENTS

The research reported here was partially supported by the U.S. Department of Energy. We are pleased to acknowledge stimulating remarks concerning the central-peak enhancement with Dr. P.D. Drummond.

APPENDIX A

In this appendix we derive the explicit expression of the second contribution S_{II} and third contribution S_{III} for the vector $S(t,\omega,\Gamma)$ in (3.3).

The formal solutions of Eqs. (2.4) and (2.8) can be written as follows:

$$\psi(t)=e^{M(t-t_0)}\psi(t_0)+\frac{1}{M}(e^{M(t-t_0)}-1)f \tag{A1}$$

and

$$\Psi(t_1,t_2)=e^{M(t_1-t_{10})}\Psi(t_{10},t_2) + \frac{1}{M}(e^{M(t_1-t_{10})}-1)F(t_2)\ , \tag{A2}$$

where $\psi(t_0)$ and $\Psi(t_{10},t_2)$ are proper initial conditions for a given type of evolution (in the field: $0\le t\le t_p$ with the matrix M; or out of the field: $t>t_p$ with the matrix M_0). Equation (A2) describes the time evolution of $\Psi(t_1,t_2)$ with respect to the first time variable only.

It is useful to note also that

$$\Psi(t_1,t_1)=T\psi(t_1)+\zeta\ , \tag{A3}$$

where

$$T=\begin{bmatrix}0 & \frac{1}{2} & 0\\ 0 & 0 & -1\\ 0 & 0 & 0\end{bmatrix},\quad \zeta=\begin{bmatrix}\frac{1}{2}\\ 0\\ 0\end{bmatrix}. \tag{A4}$$

For later reference we note that in the field we have

$$F(t_2)=MU\psi(t_2)\ , \tag{A5a}$$

where

$$U=\frac{1}{M}\begin{bmatrix}0&0&0\\0&0&-A\\0&0&0\end{bmatrix}, \tag{A5b}$$

or out of the field

$$F(t_2)=M_0U_0\psi(t_2) \tag{A6a}$$

and

$$U_0=\frac{1}{M_0}\begin{bmatrix}0&0&0\\0&0&-A\\0&0&0\end{bmatrix}=\begin{bmatrix}0&0&0\\0&0&1\\0&0&0\end{bmatrix}. \tag{A6b}$$

It is also worthwhile to notice that

$$U_0\frac{1}{M_0}f=0 \tag{A7}$$

and

$$-T\frac{1}{M_0}f+\zeta=0\,. \tag{A8}$$

We also define, for convenience,

$$\chi=\psi(0)+\frac{1}{M}f\,. \tag{A9}$$

The second contribution in (3.3) can be written as

$$S_{\rm II}(t,\omega,\Gamma)=2\Gamma e^{-\Gamma(t-t_p)}{\rm Re}\sum_{i=1}^{6}S_{\rm II}^{(i)}\,, \tag{A10}$$

with

$$S_{\rm II}^{(1)}=\frac{e^{(\Gamma/2-iD+M_0)(t-t_p)}-1}{\Gamma/2-iD+M_0}e^{-(\Gamma/2+iD-M)t_p}Q(t_p)(\chi)\,, \tag{A10a}$$

$$S_{\rm II}^{(2)}=\frac{e^{(\Gamma/2-iD+M_0)(t-t_p)}-1}{\Gamma/2-iD+M_0}e^{-(\Gamma/2+iD-M)t_p}\frac{e^{(\Gamma/2+iD-M)t_p}-1}{\Gamma/2+iD-M}\left[-(T+U)\frac{1}{M}f+\zeta\right], \tag{A10b}$$

$$S_{\rm II}^{(3)}=\frac{e^{(\Gamma/2-iD+M_0)(t-t_p)}-1}{\Gamma/2-iD+M_0}(U_0-U)\frac{e^{Mt_p}-e^{-(\Gamma/2+iD)t_p}}{\Gamma/2+iD+M}(\chi)\,, \tag{A10c}$$

$$S_{\rm II}^{(4)}=\frac{e^{(\Gamma/2-iD+M_0)(t-t_p)}-1}{\Gamma/2-iD+M_0}(U_0-U)\frac{e^{-(\Gamma/2+iD)t_p}-1}{\Gamma/2+iD}\frac{1}{M}f\,, \tag{A10d}$$

$$S_{\rm II}^{(5)}=-\frac{e^{(\Gamma/2-iD)(t-t_p)}-1}{\Gamma/2-iD}U_0\frac{e^{Mt_p}-e^{-(\Gamma/2+iD)t_p}}{\Gamma/2+iD+M}(\chi)\,, \tag{A10e}$$

$$S_{\rm II}^{(6)}=-\frac{e^{(\Gamma/2-iD)(t-t_p)}-1}{\Gamma/2-iD}U_0\frac{e^{-(\Gamma/2+iD)t_p}-1}{\Gamma/2+iD}\frac{1}{M}f\,, \tag{A10f}$$

where we have defined

$$Q(t_p)=\int_0^{t_p}dt_2e^{(\Gamma/2+iD-M)t_2}(T+U)e^{Mt_2}\,. \tag{A11}$$

The third contribution in (3.3) is

$$S_{\rm III}(t,\omega,\Gamma)={\rm Re}\sum_{i=1}^{4}S_{\rm III}^{(i)} \tag{A12}$$

with

$$S_{\rm III}^{(1)}=\frac{2\Gamma}{\Gamma/2-iD+M_0}e^{-(\Gamma/2+iD-M_0)(t-t_p)}P(t-t_p)R(t_p)\,, \tag{A12a}$$

$$S_{\rm III}^{(2)}=\frac{-2\Gamma}{\Gamma/2-iD+M_0}e^{-\Gamma(t-t_p)}(T+U_0)\frac{e^{(\Gamma+M_0)(t-t_p)}-1}{\Gamma+M_0}R(t_p)\,, \tag{A12b}$$

$$S_{\rm III}^{(3)}=\frac{-2\Gamma}{\Gamma/2-iD}e^{-(\Gamma/2+iD)(t-t_p)}U_0\frac{e^{(\Gamma/2+iD+M_0)(t-t_p)}-1}{\Gamma/2+iD+M_0}R(t_p)\,, \tag{A12c}$$

$$S_{\rm III}^{(4)}=\frac{2\Gamma}{\Gamma/2-iD}e^{-\Gamma(t-t_p)}U_0\frac{e^{(\Gamma+M_0)(t-t_p)}-1}{\Gamma+M_0}R(t_p)\,, \tag{A12d}$$

where we have denoted

$$P(t-t_p)=\int_0^{t-t_p} dt_2 e^{(\Gamma/2+iD-M_0)t_2}(T+U_0)e^{M_0 t_2} \tag{A13}$$

and

$$R(t_p)=\psi(t_p)+\frac{1}{M_0}f$$
$$=e^{Mt_p}\psi(0)+\frac{1}{M}(e^{Mt_p}-1)f+\frac{1}{M_0}f\ . \tag{A14}$$

We have used (A7) and (A8) to eliminate four more terms which formally appear in (A14). Because of the structure of the matrix U_0, given by (A6), with all zeros in the first row, the terms with U_0 in Eqs. (A10) and (A12) will not contribute to the spectrum, which is the first component of the vector $S(t,\omega,\Gamma)$, and we can drop them. These formulas describe the physical spectrum of delayed resonance fluorescence for any duration of the laser pulse t_p and any delay time $t-t_p$. Using these formulas the spectrum can be easily plotted by a computer.

---

*Also with Department of Chemistry, University of Rochester; permanent address: Institute of Physics, Academia Sinica, Beijing, The People's Republic of China.

†Permanent address: Institute of Physics, A. Mickiewicz University, Grunwaldzka 6, 60-780 Poznań, Poland.

[1]J. H. Eberly and K. Wódkiewicz, J. Opt. Soc. Am. 67, 1252 (1977).

[2]J. H. Eberly, C. V. Kunasz, and K. Wódkiewicz, J. Phys. B 13, 217–239 (1980).

[3]P. W. Milonni, Ph.D. thesis, University of Rochester, 1974 (unpublished).

[4]B. R. Mollow, Phys. Rev. 188, 1969 (1969), first considered the two-level spectrum with purely radiative relaxation. See also M. Newstein, Phys. Rev. 167, 89 (1968), and A. I. Burshtein, Zh. Eksp. Teor. Phys. 49, 1362 (1965) [Sov. Phys.—JETP 22, 939 (1966)].

[5]The appearance of a *difference* of widths $\Gamma-A$, instead of a sum $\Gamma+A$, in the resonant denominator has been widely mentioned recently in connection with so-called "subnatural linewidth" spectroscopy. See, for example, the discussion, with many references, given by P. L. Knight, Comments At. Mol. Physics X, 241 (1981).

[6]P. Saari, in *Light Scattering in Solids,* edited by J. L. Birman, H. Z. Cummins, and K. K. Rebane, (Plenum, New York, 1979), pp. 315–329.

[7]E. Courtens and A. Szöke, Phys. Rev. A 15, 1588 (1977).

[8]P. F. Williams, D.L. Rousseau, and S. H. Dworetsky, Phys. Rev. Lett. 32, 196 (1974).

[9]P. L. Knight, W. A. Molander, and C. R. Stroud, Jr., Phys. Rev. A 17, 1547 (1978).

[10]M. G. Raymer and J. Cooper, Phys. Rev. A 20, 2238 (1979).

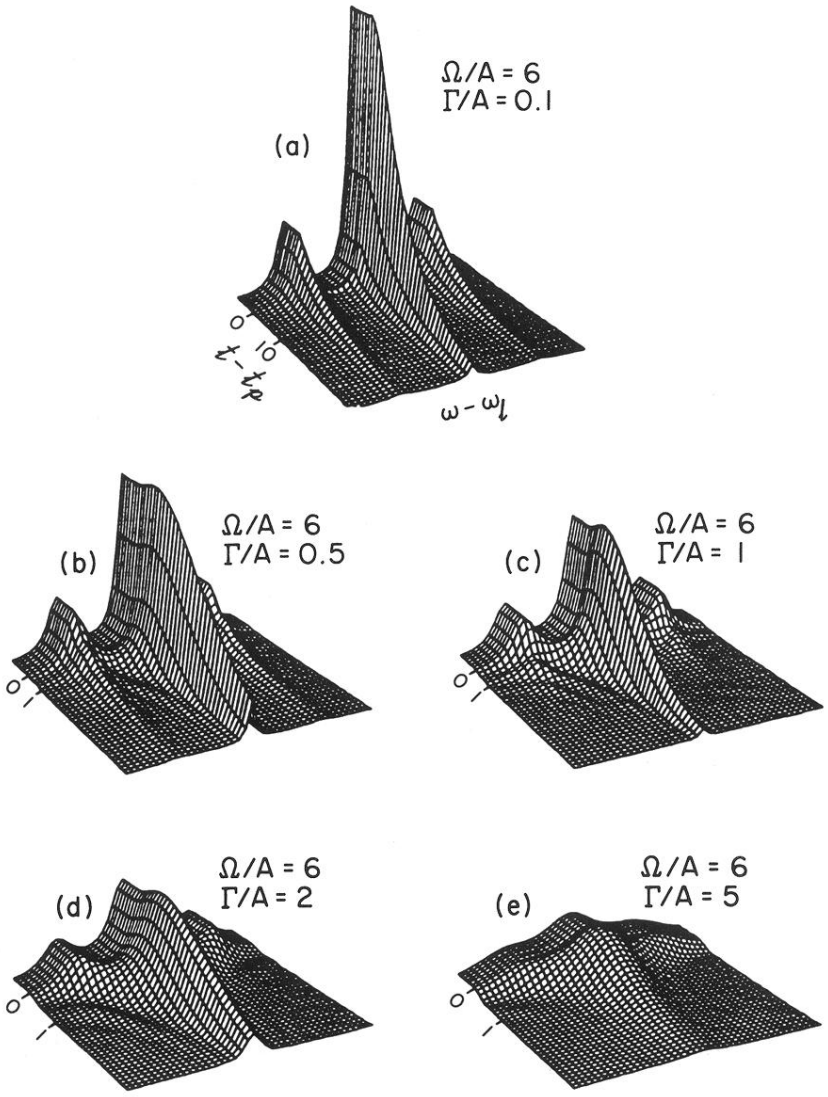

FIG. 3. Dealyed resonance fluorescence spectrum for $\Omega/A=6$ and different values of Γ/A: (a) $\Gamma/A=0.1$, (b) $\Gamma/A=0.5$, (c) $\Gamma/A=1$, (d) $\Gamma/A=2$, (e) $\Gamma/A=5$. First few lines in the time direction represent the steady-state spectrum for easier reference. Time is in units of A^{-1}. Labeling of the curves in graph (a) applies to (b)—(e).

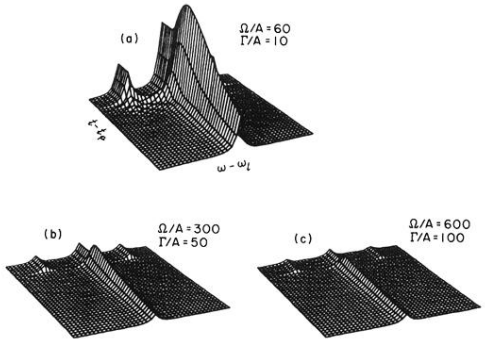

FIG. 5. Spectrum obtained using a broad-band interferometer for different values of parameters: (a) $\Omega/A=60$, $\Gamma/A=10$; (b) $\Omega/A=300$, $\Gamma/A=50$; (c) $\Omega/A=600$, $\Gamma/A=100$. Amplitude scale has been multiplied by a factor of 5 as compared to Fig. 3. The labeling of the curves in (a) applies to (b) and (c).